

# Time-Domain Electromagnetic Inversion Technique for Biological Tissues by Reconstructing Distributions of Cole-Cole Model Parameters

Guangdong Liu

School of Physics and Electronic Engineering  
Fuyang Normal University, Fuyang, 236037, China  
liu\_guang\_dong@126.com

**Abstract** — The Cole-Cole (C-C) models have been frequently used for a precise description of the dispersion characteristics of biological tissues. One of the main difficulties in the direct reconstruction of these dielectric properties from time-domain measurements is their frequency dependence. In order to overcome this difficulty, an electromagnetic (EM) inversion technique in the time domain is proposed, in which four kinds of frequency-independence model parameters, the optical relative permittivity, the static conductivity, the relative permittivity difference, and the relaxation time, can be determined simultaneously. It formulates the inversion problem as a regularized minimization problem, whose forward and backward subproblems could be solved iteratively by the finite-difference time-domain (FDTD) method and any conjugate gradient algorithm, respectively. Numerical results on two types of stratified C-C slabs, with smooth and discontinuous parameter profiles, respectively, confirm the performance of the inversion methodology.

**Index Terms** — Biological tissues, conjugate gradient methods, electromagnetic scattering by dispersive media, electromagnetic scattering inverse problems, finite-difference time-domain (FDTD) methods, regulators.

## I. INTRODUCTION

The electromagnetic (EM) inverse scattering problems, which aim to estimate the EM properties from the measurements outside the object of interest, have attracted increasing attention recently, due to their extensive application fields, and some promising results [1-3]. Nevertheless, in general, there are two major difficulties for these problems: one difficulty is their nonlinearity, and the other is the non-uniqueness of their solution [4].

Methodologically, the EM scattering inverse problem may be solved in the frequency domain [5] or the time domain [6]. By contrast, the time-domain reconstructed results are better than those by applying any single-frequency technique in the amount of information and the resolution of images [1, 6, 7]. Currently, several

inversion approaches in the time domain for nondispersive media have been developed, such as the forward-backward time-stepping (FBTS) method [8] and the Lagrange multipliers technique [9]. However, in the real world, the wideband dielectric properties of biological tissues are dispersive, which have been widely described by the Debye or Cole-Cole (C-C) models, but the precision of the former is not better than that of the latter [10]. One basic difficulty in the time-domain reconstruction of the electrical characteristics is their frequency correlation. To date, a few time-domain inversion methods for Debye media have been proposed [6, 11]. Unfortunately, for C-C frequency-dependent media, the existing methods are not suitable, and few inverse methods are available directly.

Recently, several finite-difference time-domain (FDTD) forward solvers suitable for C-C media have been presented [12, 13], which have laid the groundwork for the research of inverse solvers for this class of media. There are two novelties in this paper. One novelty is to present a new inverse EM scattering technique, which is to reconstruct the C-C model parameters by means of measurements in the time domain directly. And the other innovation is to introduce a regularization scheme to cope with the ill-posedness of the inverse problem, which was not used in references [1, 6, 11].

## II. INVERSE SCATTERING TECHNIQUE IN THE TIME DOMAIN

### A. Problem formulation

Suppose that a problem space  $V$ , occupied by some biological tissues, is surrounded by a region  $D$ , filled with a known background medium. Also, it is assumed that all the media are linear, isotropic, and nonmagnetic, and that the complex-valued relative permittivity,  $\epsilon_r^*$ , of the media within  $V$  is modeled by the single pole C-C electrical dispersion equation as [10]:

$$\epsilon_r^*(\omega) = \epsilon_\infty - j\sigma_s / (\omega\epsilon_0) + \Delta\epsilon / [1 + (j\omega\tau)^\alpha], \quad (1)$$

where  $\Delta\epsilon = \epsilon_s - \epsilon_\infty$ ,  $\epsilon_s$  and  $\epsilon_\infty$  are the static and optical relative permittivity, respectively,  $\sigma_s$  is the static

conductivity,  $\tau$  and  $\alpha$  ( $0 \leq \alpha \leq 1$ ) denote the relaxation time and the dispersion breadth, respectively,  $j^2 = -1$ ,  $\epsilon_0$  is the dielectric constant of free space, and  $\omega$  represents the angular frequency.

For simplicity, we assume that  $\alpha$  is *a priori* known (it is appropriate for most biological tissues since they are not distinctly different in a wide frequency range [10]).

Our objective is therefore to determine four kinds of unknowns, ( $\epsilon_\infty$ ,  $\sigma_s$ ,  $\Delta\epsilon$ , and  $\tau$ ), for every position within  $V$ . These C-C model parameters can be explicitly shown in the following field equations when activating the  $i^{\text{th}}$  incidence for the time interval  $[0, T]$ :

$$\nabla \times \mathbf{E}_i + \mu_0 \partial_t \mathbf{H}_i = \mathbf{0}, \quad (2)$$

$$\nabla \times \mathbf{H}_i - \epsilon_0 \epsilon_\infty \partial_t \mathbf{E}_i - \sigma_s \mathbf{E}_i - \mathbf{J}_i - \mathbf{J}_i^s = \mathbf{0}, \quad (3)$$

and a fractional auxiliary differential equation (ADE) [13]:

$$\mathbf{J}_i + \tau^\alpha \mathbf{D}_t^\alpha \mathbf{J}_i - \epsilon_0 \Delta \partial_t \mathbf{E}_i = \mathbf{0}, \quad (4)$$

where  $\mu_0$  is the free-space permeability,  $\mathbf{E}_i$ ,  $\mathbf{H}_i$ , and  $\mathbf{J}_i$  are the electric field intensity, magnetic field intensity, and dispersion current, respectively,  $\mathbf{J}_i^s$  is the current density,  $\nabla$  is the Hamilton operator, and  $\partial_t$  and  $\mathbf{D}_t^\alpha$  denote 1<sup>st</sup>-order and  $\alpha^{\text{th}}$ -order temporal partial differential operators with respect to time variable,  $t$ , respectively.

### B. Constrained minimization problem

In order to cope with the nonlinearity of the aforementioned inverse problem, we formulate it as a constrained minimization problem:

$$\begin{cases} \mathbf{p} = \arg \min_{\mathbf{p}} [F(\mathbf{p})], \\ \text{s.t. (2)–(4)}, \end{cases} \quad (5)$$

where the estimated parameters  $\mathbf{p} = [\epsilon_\infty, \sigma_s, \Delta\epsilon, \tau]^T$ , and the cost functional  $F$  is given by:

$$\begin{aligned} F = & \frac{1}{2} \sum_{i=1}^I \sum_{j=1}^J \int_0^T \|\mathbf{E}_{ij}(\mathbf{p}) - \mathbf{E}_{ij}^{\text{mea}}\|_2^2 dt \\ & + \frac{1}{2} \sum_{m=1}^4 \int_V \gamma_m \|\nabla p_m\|_2^2 dv. \end{aligned} \quad (6)$$

In the right hand side of (6), the first term formulates inversion error, in which  $\mathbf{E}_{ij}$  and  $\mathbf{E}_{ij}^{\text{mea}}$  represent the calculated and measured electric fields at the  $j^{\text{th}}$  receiving position due to the  $i^{\text{th}}$  incident wave, respectively, and  $I$  and  $J$  denote the total number of transmitters and receivers, respectively. While the second term, which is not contained in references [1, 6, 11], is incorporated to regularize the ill-posedness of the inverse problem, in which  $\gamma_m$  ( $m = 1, 2, 3, 4$ ) are four positive Tikhonov regularization factors.

### C. Unconstrained minimization problem

Based on the method of the Lagrange penalty function, the above constrained minimization problem is

turned into an unconstrained minimization one, whose augmented cost functional  $F^a$  is represented as:

$$\begin{aligned} F^a = & \sum_{i=1}^I \int_0^T \int_V \left[ \mathbf{e}_i \cdot (\nabla \times \mathbf{H}_i - \epsilon_0 \epsilon_\infty \partial_t \mathbf{E}_i - \sigma_s \mathbf{E}_i - \mathbf{J}_i - \mathbf{J}_i^s) \right. \\ & + \mathbf{h}_i \cdot (\nabla \times \mathbf{E}_i + \mu_0 \partial_t \mathbf{H}_i) \\ & \left. + \mathbf{q}_i \cdot (\mathbf{J}_i + \tau^\alpha \mathbf{D}_t^\alpha \mathbf{J}_i - \epsilon_0 \Delta \partial_t \mathbf{E}_i) \right] dv dt + F, \end{aligned} \quad (7)$$

where  $\mathbf{e}_i$ ,  $\mathbf{h}_i$ , and  $\mathbf{q}_i$  are the Lagrange vector multipliers.

### D. Fréchet derivatives

Solving (7) by the variational method [14], we have  $\delta F^a = 0$ , where  $\delta$  denotes the first-order variation operator. After some calculus of variations similar to [1, 6, 11], it can be derived that the fields  $\mathbf{e}_i$ ,  $\mathbf{h}_i$ , and  $\mathbf{j}_i$  ( $\mathbf{j}_i =: -\epsilon_0 \Delta \partial_t \mathbf{q}_i$ ) must satisfy the following equations for the time interval  $[T, 0]$ :

$$\nabla \times \mathbf{e}_i - \mu_0 \partial_t \mathbf{h}_i = \mathbf{0}, \quad (8)$$

$$\nabla \times \mathbf{h}_i + \epsilon_0 \epsilon_\infty \partial_t \mathbf{e}_i - \sigma_s \mathbf{e}_i - \mathbf{j}_i + \sum_{j=1}^J (\mathbf{E}_{ij} - \mathbf{E}_{ij}^{\text{mea}}) = \mathbf{0}, \quad (9)$$

$$\mathbf{j}_i - \tau^\alpha \mathbf{D}_t^\alpha \mathbf{j}_i + \epsilon_0 \Delta \partial_t \mathbf{e}_i = \mathbf{0}, \quad (10)$$

and that the Fréchet derivatives (gradients) of  $F^a$  with respect to  $p_m$  are denoted as:

$$g_{\epsilon_\infty} =: \delta F^a / \delta \epsilon_\infty = -\epsilon_0 \sum_{i=1}^I \int_0^T (\mathbf{e}_i \cdot \partial_t \mathbf{E}_i) dt - \gamma_1 \nabla^2 \epsilon_\infty, \quad (11)$$

$$g_{\sigma_s} =: \delta F^a / \delta \sigma_s = -\sum_{i=1}^I \int_0^T (\mathbf{e}_i \cdot \mathbf{E}_i) dt - \gamma_2 \nabla^2 \sigma_s, \quad (12)$$

$$\begin{aligned} g_{\Delta\epsilon} =: & \delta F^a / \delta \Delta\epsilon = \\ & - \left[ \sum_{i=1}^I \int_0^T (\mathbf{j}_i \cdot \mathbf{E}_i) dt / \Delta\epsilon \right] - \gamma_3 \nabla^2 \Delta\epsilon, \end{aligned} \quad (13)$$

$$\begin{aligned} g_\tau =: & \frac{\delta F^a}{\delta \tau} = \left[ \alpha \tau^{\alpha-1} \sum_{i=1}^I \int_0^T (\mathbf{D}_t^{1-\alpha} \mathbf{j}_i \cdot \mathbf{J}_i) dt / (\epsilon_0 \Delta\epsilon) \right] \\ & - \gamma_4 \nabla^2 \tau, \end{aligned} \quad (14)$$

where  $\mathbf{D}_t^{1-\alpha}$  indicates a fractional differential operator, whose numerical treatment could be found in [15], the direct fields ( $\mathbf{E}_i$ ,  $\mathbf{H}_i$ , and  $\mathbf{J}_i$ ) and the adjoint fields ( $\mathbf{e}_i$ ,  $\mathbf{h}_i$ , and  $\mathbf{j}_i$ ) can be calculated by using the FDTD method based on approximation of the Grünwald-Letnikov fractional derivative, from (2)–(4) and (8)–(10), respectively [13].

### E. Inversion algorithm

In this work, we select the Polak-Ribière-Polyak conjugate gradient algorithm [16] to solve the derived problem. Let the discretized forms of the C-C model parameters and gradients be represented by:

$$\mathbf{x} = [\epsilon_\infty^1, \dots, \epsilon_\infty^N, \sigma_s^1, \dots, \sigma_s^N, \Delta\epsilon^1, \dots, \Delta\epsilon^N, \tau^1, \dots, \tau^N]^T, \quad (15)$$

and

$$\mathbf{g} = \left[ g_{\sigma_s^1}, \dots, g_{\sigma_s^N}, g_{\sigma_s^1}, \dots, g_{\sigma_s^N}, \right. \\ \left. g_{\Delta\epsilon^1}, \dots, g_{\Delta\epsilon^N}, g_{\tau^1}, \dots, g_{\tau^N} \right]^T, \quad (16)$$

respectively. Given that the estimated value of  $\mathbf{x}$  at the  $k^{\text{th}}$  iteration,  $\mathbf{x}_k$ , is achieved, the next estimated  $\mathbf{x}_{k+1}$  is updated by:

$$\mathbf{x}_{k+1} = \mathbf{x}_k + \lambda_k \mathbf{d}_k, \quad (17)$$

where  $\lambda_k$  is the step size, and the direction  $\mathbf{d}_k$  is given by [16]:

$$\mathbf{d}_k = \begin{cases} -\mathbf{g}_k, & (k=1), \\ -\mathbf{g}_k + \frac{\mathbf{g}_k^T \cdot (\mathbf{g}_k - \mathbf{g}_{k-1})}{\mathbf{g}_{k-1}^T \cdot \mathbf{g}_{k-1}} \mathbf{d}_{k-1}, & (k \geq 2), \end{cases} \quad (18)$$

where  $\mathbf{g}_k$  denotes the estimated value of  $\mathbf{g}$  at the  $k^{\text{th}}$  iteration.

At the  $k^{\text{th}}$  iteration, the relative mean square error  $e$  between the true parameters  $\mathbf{x}$  and estimated ones  $\mathbf{x}_k$  is defined as:

$$e(k) = \|\mathbf{x} - \mathbf{x}_k\|_2 / \|\mathbf{x}\|_2. \quad (19)$$

The above inverse problem is solved iteratively until a predetermined error threshold  $e_{\text{th}}$  is reached or a predefined iteration number  $k_{\text{pre}}$  is finished. The basic steps of the inversion algorithm are illustrated in Fig. 1.

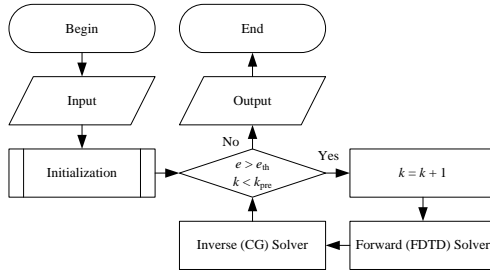


Fig. 1. Basic flow-chart of the proposed inversion technology.

### III. NUMERICAL RESULTS AND DISCUSSION

In this section, two simple one-dimensional (1-D) numerical examples, similar to [1, 6], are provided to examine the performance of the newly-elaborated approach. The geometry of the examples is shown in Fig. 2, in which either side of a  $4d$ -width objective region is surrounded by a known background medium (air) where  $d = 10$  mm, and all their electrical properties depend only on  $z$  coordinate, where the positive direction of  $z$  axis is from left to right, and  $z = 0$  is on the left plane of the left background medium.

The objective region consists of layered C-C medium with a parameter of  $\alpha = 0.8$ . In the background medium, a bistatic detection system is applied where two transmitters ( $I = 2$ ), denoted by T, are symmetrically

placed at distance equal to  $d/2$  from both sides of the objective region, while two receivers ( $J = 2$ ), denoted by R, are placed at symmetrical distance equal to  $d/4$  from both sides of the objective region. An ultra-wideband pulse of the excitation source for transmitters is selected the same as [12]:

$$s(t) = \sin(2\pi f_c(t - 4/a)) \exp(-a^2(t - 4/a)^2), \quad (20)$$

where  $a = 1.26 \times 10^{10}$ , and central frequency  $f_c = 3$  GHz.

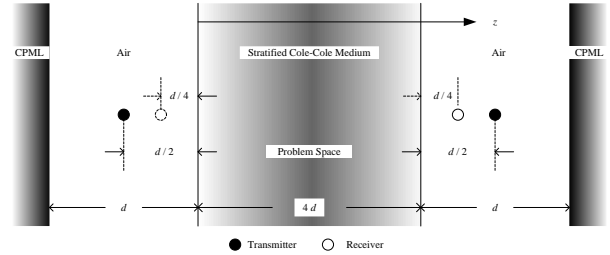


Fig. 2. Geometry model of 1-D problem.

The FDTD method is applied to compute the direct and adjoint fields [13]. The FDTD solution space, which is bounded by the five-cell convolution perfectly matched layer (CPML) [17], consists of 120 homogeneous cells with spatial size  $\Delta z = 0.5$  mm and time step  $\Delta t = 0.5\Delta z/c_0$ , where  $c_0$  is the speed of light in free space. Therefore, the total number of unknowns is 320. In this work, the necessary measurement data came from the similar FDTD simulation with  $T = 1500\Delta t$ , but its cell size is twice finer than the one used in the inverse solver to avoid the ‘‘inverse crime’’.

Besides, it is assumed that the location and width of the reconstruction region are *a priori* known, that a set of values (6.0, 0.5 S·m<sup>-1</sup>, 20.0, and 7.0 ps), which are the average values of the C-C model parameters ( $\epsilon_s$ ,  $\sigma_s$ ,  $\Delta\epsilon$ , and  $\tau$ ) within the objective region, is selected as an initial guess of the inversion algorithm, and that the specific stopping condition for the iterative algorithm is that reconstruction errors are not declining or  $k_{\text{pre}} = 30$ .

In the first example, the spatial distribution profiles of the four parameters within the entire objective region are smooth (sinusoidal or cosinusoidal), whose (peaks, valleys) for  $\epsilon_s$ ,  $\sigma_s$ ,  $\Delta\epsilon$ , and  $\tau$  are (10.0, 2.0), (0.9 S·m<sup>-1</sup>, 0.1 S·m<sup>-1</sup>), (30.0, 10.0), and (8.0 ps, 6.0 ps), respectively.

Firstly, the regularization term is not applied in the noiseless case (i.e., set  $\gamma_m = 0$  with  $m = 1, 2, 3, 4$ ). After 30 iterations, the estimated optical relative permittivity, static conductivity, relative permittivity difference, and relaxation time are obtained as shown in subfigures (a)–(d) of Fig. 3. In these subfigures, the solid black lines, small red dots, and small blue circles depict the true distributions, start values, and end values, respectively (similarly for the later cases).

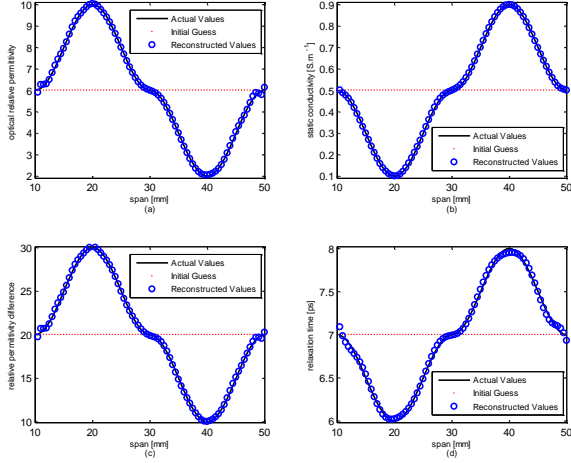


Fig. 3. The reconstructed distributions of: (a) optical relative permittivity, (b) static conductivity, (c) relative permittivity difference, and (d) relaxation time for a stratified Cole-Cole slab with smooth model parameter profiles, using noiseless data without regularization, at the 30<sup>th</sup> iteration. For comparison purpose, its corresponding original distributions with smooth profiles, and homogeneous initial guess are given, too (similarly for later cases).

As can be seen in Fig. 3, the proposed method for the non-regularized 1-D problem is convergent when noise is not considered, and that all the model parameters of the C-C dispersive media are reconstructed precisely.

Secondly, it is assumed that the measured fields are corrupted by the additive white Gaussian noise (AWGN) with a signal-to-noise ratio (SNR) of 20 dB. The same procedures as the previous case are repeated, where no regularization scheme is adopted yet. Numerical experiments show that the reconstruction errors are not decreased just after 14 iterations. The estimated optical relative permittivity, static conductivity, relative permittivity difference, and relaxation time are obtained as illustrated in subfigures (a)–(d) of Fig. 4 at the 14<sup>th</sup> iteration, where the estimated relative mean square error is about 0.25.

From Fig. 4, it is obvious that all the estimated distributions are poor, especially for the optical relative permittivity and relaxation time.

Finally, suppose that the simulated measurement field data are corrupted by the AWGN with a SNR of 20 dB, too. To test the performance of the regularized inversion algorithm, four of regularization factors ( $\gamma_1$ ,  $\gamma_2$ ,  $\gamma_3$ , and  $\gamma_4$ ) are chosen to be (0.01, 0.001, 0.01, and 0.0001), respectively. It is noteworthy that these factors could be not optimal. The estimated optical relative permittivity, static conductivity, relative permittivity difference, and relaxation time are obtained as given in subfigures (a)–(d) of Fig. 5 at 30<sup>th</sup> iteration.

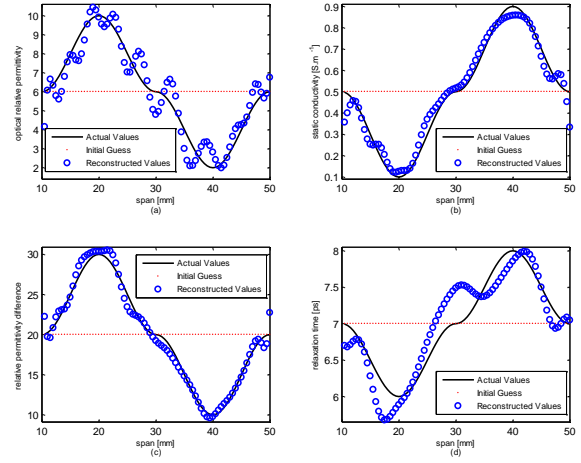


Fig. 4. The reconstructed distributions of: (a) optical relative permittivity, (b) static conductivity, (c) relative permittivity difference, and (d) relaxation time for a stratified Cole-Cole slab with smooth model parameter profiles, applying noisy data (SNR = 20 dB) without regularization, at the 14<sup>th</sup> iteration.

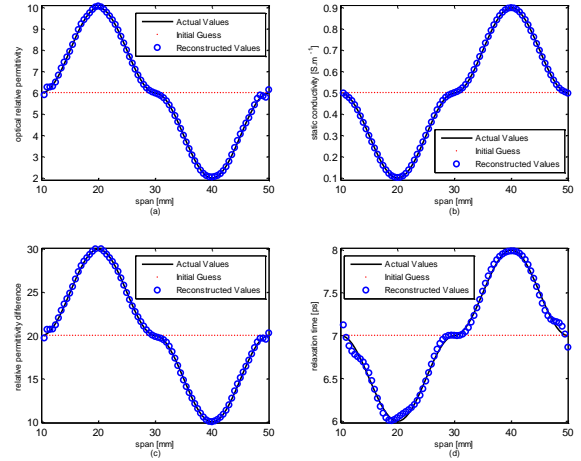


Fig. 5. The reconstructed distributions of: (a) optical relative permittivity, (b) static conductivity, (c) relative permittivity difference, and (d) relaxation time for a stratified Cole-Cole slab with smooth model parameter profiles, using noisy data (SNR = 20 dB) with regularization, at the 30<sup>th</sup> iteration.

Figure 5 shows that the recreated model parameters of the C-C dispersive media are satisfactory, even based on the noise-contaminated data with a SNR of 20 dB, which could benefit from the additional regularization terms.

In addition, the relative mean square errors versus the number of iterations, for the first and last cases, are presented in Fig. 6, where the final values of the errors are approximately 0.052 and 0.057, respectively.

Figure 6 indicates clearly that the proposed method is convergent, and the relative mean square errors are decreased with the increase of the number of iterations in two cases, and that the final error in the last case is slightly larger than that in the first case.

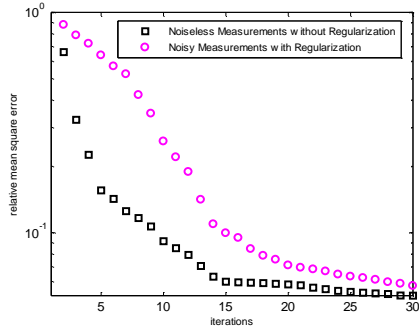


Fig. 6. In the iterative inversion methodology, relative mean square errors versus the number of iterations.

The second example is to reconstruct an inhomogeneous C-C slab with discontinuous (step-shaped) model parameter profiles, consisting of six layers. The width of the second and fifth layers is all 10 mm, and that of other layers is all 5 mm. The parameters ( $\epsilon_\infty$ ,  $\sigma_s$ ,  $\Delta\epsilon$ , and  $\tau$ ) of the first and third layers are all (8.0, 0.3 S·m<sup>-1</sup>, 25.0, and 6.5 ps), those of the second layer are (10.0, 0.9 S·m<sup>-1</sup>, 30.0, and 6.0 ps), those of the fourth and sixth layers are all (4.0, 0.7 S·m<sup>-1</sup>, 15.0, and 7.5 ps), and those of the fifth layer are (2.0, 0.9 S·m<sup>-1</sup>, 10.0, and 8.0 ps).

After 30 iterations of the algorithm with regularization (regularization factors are the same as the first example) based on a noisy scenario (SNR is the same as the first example, too), the estimated optical relative permittivity, static conductivity, relative permittivity difference, and relaxation time are obtained as shown in subfigures (a)–(d) of Fig. 7. The error at the 30<sup>th</sup> iteration is about 0.16.

Figure 7 shows that even when the distributions of the C-C model parameters for a slab are discontinuous and the simulated measurements are added a noise with a SNR of 20 dB, the inversion algorithm is still convergent, and the reconstructed results are acceptable. Note that the final error in the discontinuous case is noticeably larger than that in the smooth one.

Theoretically, the initial guess applied in the inversion algorithm could be also important to its imaging performance. For this reason, the inversion algorithm is applied to the third case of the first example, the only difference is that the initial guess is replaced with the C-C model parameters of the known background medium (air), (1.0, 0.0 S·m<sup>-1</sup>, 0.0, and 8.0 ps). The reconstructed optical relative permittivity, static conductivity, relative permittivity difference, and

relaxation time are presented in subfigures (a)–(d) of Fig. 8. The error at the 30<sup>th</sup> iteration is approximately 0.063.

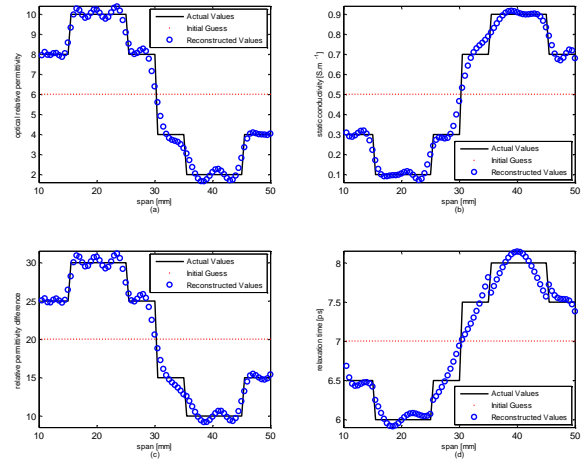


Fig. 7. The reconstructed distributions of: (a) optical relative permittivity, (b) static conductivity, (c) relative permittivity difference, and (d) relaxation time for a stratified Cole-Cole slab with discontinuous model parameter profiles, using noisy data (SNR = 20 dB) with regularization, at the 30<sup>th</sup> iteration.

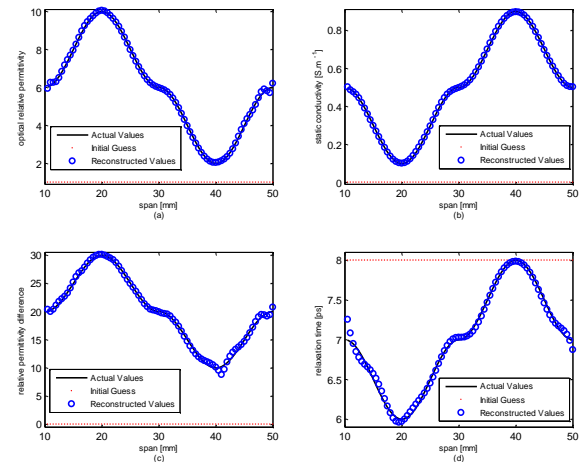


Fig. 8. The reconstructed distributions of: (a) optical relative permittivity, (b) static conductivity, (c) relative permittivity difference, and (d) relaxation time for a stratified Cole-Cole slab with smooth model parameter profiles, using noisy data (SNR = 20 dB) with regularization, at the 30<sup>th</sup> iteration.

Figure 8 shows that the reconstructed C-C model parameters are also acceptable, based on the new initial guess. Thus, the proposed method is robust to initial guess.

The whole solution program codes written in MATLAB (R2011b, win64-bit) are iteratively executed

on a PC with a four-core i5-2320 CPU, each iteration taking, on average, about 2.87 s.

As previously mentioned, the nonlinearity and ill-posedness are two major difficulties in the solution of the inverse problem. Indeed, in order to bridge over the first difficulty, two similar multi-frequency time-harmonic imaging approaches, the frequency-hopping approach [18] and the simultaneous inversion one [19], have been proposed. While the time-domain technique presented in this paper is a natural extension from several frequencies to an entire frequency range, which could produce imaging results with higher resolution and accuracy. When this time-domain technique is, however, applied to large scale problems such as high-dimensional ones, their high computational cost will become a new difficulty, which may be overcome by either of the multi-frequency methods.

For the second difficulty, the Tikhonov regularization scheme used in this work is one of remedies, in which the reasonable regularization parameters (factors  $\gamma_m$ ) for a particular problem can be determined by several regularization parameter-choice techniques such as the L-curve method [20]. Naturally, it will add additional computational cost to the problem. Besides, other regularization schemes, such as the total variation (TV) regularization [21], can also be adopted to remedy the ill-posedness of the inverse problem.

#### IV. CONCLUSION

This paper estimates four frequency-dependent parameters in the single pole Cole-Cole electrical dispersion equation via a time-domain optimization method. The first contribution in the developed inversion technique is direct reconstruction of four sorts of parameters for the C-C dispersive media from the time-domain measured data. The second one is that comparative studies on the same 1-D problem in three different cases are carried out. The numerical results demonstrate that the proposed technique is feasible for quantitative determination of the parameters of the 1-D example, and it provides a valuable tool for microwave imaging of biological tissues. The further work is to investigate multidimensional reconstruction problems as well as else regularization schemes.

#### ACKNOWLEDGMENT

This work was supported in part by the National Natural Science Foundation of China under Grant No. 51271059, the Key Program of the Natural Science Foundation of Anhui Higher Education Institutions of China under Grant No. KJ2014A193, the Science and Technology Program of Anhui Province of China under Grant No. 1604a0702037, and the Teaching Research Program of Fuyang Normal University under Grant No. 2015JYXM35.

#### REFERENCES

- [1] T. G. Papadopoulos and I. T. Rekanos, "Estimation of the parameters of Lorentz dispersive media using a time-domain inverse scattering technique," *IEEE Trans. Magn.*, vol. 48, no. 2, pp. 219-222, Feb. 2012.
- [2] F. Bai, A. Franchois, and A. Pizurica, "3D microwave tomography with Huber regularization applied to realistic numerical breast phantoms," *Progress In Electromagnetics Research*, vol. 155, pp. 75-91, 2016.
- [3] M. T. Bevacqua and R. Scapaticci, "A compressive sensing approach for 3D breast cancer microwave imaging with magnetic nanoparticles as contrast agent," *IEEE Trans. Med. Imag.*, vol. 35, no. 2, pp. 665-673, Feb. 2016.
- [4] D. Colton and R. Kress, *Inverse Acoustic and Electromagnetic Scattering Theory*. Berlin: Springer-Verlag, 1992.
- [5] W. Zhang and Q. H. Liu, "Three-dimensional scattering and inverse scattering from objects with simultaneous permittivity and permeability contrasts," *IEEE Trans. Geosci. Remote Sens.*, vol. 53, no. 1, pp. 429-439, Jan. 2015.
- [6] T. G. Papadopoulos and I. T. Rekanos, "Time-domain microwave imaging of inhomogeneous Debye dispersive scatterers," *IEEE Trans. Antennas Propagat.*, vol. 60, no. 2, pp. 1197-1202, Feb. 2012.
- [7] I. T. Rekanos and A. Räsänen, "Microwave imaging in the time domain of buried multiple scatterers by using an FDTD-based optimization technique," *IEEE Trans. Magn.*, vol. 39, no. 3, pp. 1381-1384, May 2003.
- [8] T. Takenaka, H. Jia, and T. Tanaka, "Microwave imaging of electrical property distributions by a forward-backward time-stepping method," *J. Electromagn. Waves Appl.*, vol. 14, no. 12, pp. 1609-1626, 2000.
- [9] I. T. Rekanos, "Time-domain inverse scattering using Lagrange multipliers: An iterative FDTD-based optimization technique," *J. Electromagn. Waves Appl.*, vol. 17, no. 2, pp. 271-289, 2003.
- [10] S. Gabriel, R. W. Lau, and C. Gabriel, "The dielectric properties of biological tissues. III. Parametric models for the dielectric spectrum of tissues," *Phys. Med. Biol.*, vol. 41, no. 11, pp. 2271-2293, Nov. 1996.
- [11] D. W. Winters, E. J. Bond, B. D. V. Veen, and S. C. Hagness, "Estimation of frequency-dependent average dielectric properties of breast tissue using a time-domain inverse scattering technique," *IEEE Trans. Antennas Propag.*, vol. 54, no. 11, pp. 3517-3528, Nov. 2006.
- [12] I. T. Rekanos and T. G. Papadopoulos, "An

- auxiliary differential equation method for FDTD modeling of wave propagation in Cole-Cole dispersive media," *IEEE Trans. Antennas Propag.*, vol. 58, no. 11, pp. 3666-3674, Nov. 2010.
- [13] I. T. Rekanos and T. V. Yioultis, "Approximation of Grünwald-Letnikov fractional derivative for FDTD modeling of Cole-Cole media," *IEEE Trans. Magn.*, vol. 50, no. 2, pp. 7004304, Feb. 2014.
- [14] H. Sagan, *Introduction to the Calculus of Variations*. New York, NY: McGraw-Hill, 1969.
- [15] M. Dalir and M. Bashour, "Applications of fractional calculus," *Applied Mathematical Sciences*, vol. 4, no. 21, pp. 1021-1032, 2010.
- [16] Y. H. Dai, "A family of hybrid conjugate gradient methods for unconstrained optimization," *Math. Comput.*, vol. 72, no. 243, pp. 1317-1328, Feb. 2003.
- [17] J. A. Roden and S. D. Gedney, "Convolution PML (CPML): An efficient FDTD implementation of the CFS-PML for arbitrary media," *Microw. Opt. Technol. Lett.*, vol. 27, no. 5, pp. 334-339, Dec. 2000.
- [18] W. C. Chew and J. H. Lin, "A frequency-hopping approach for microwave imaging of large inhomogeneous bodies," *IEEE Microw. Guided Wave Lett.*, vol. 5, no. 12, pp. 439-441, Dec. 1995.
- [19] Q. Fang, P. M. Meaney, and K. D. Paulsen, "Microwave image reconstruction of tissue property dispersion characteristics utilizing multiple-frequency information," *IEEE Trans. Microw. Theory Tech.*, vol. 52, no. 8, pp. 1866-1875, Aug. 2004.
- [20] P. R. Johnston and R. M. Gulrajani, "Selecting the corner in the L-curve approach to Tikhonov regularization," *IEEE Trans. Biomed. Eng.*, vol. 47, no. 9, pp. 1293-1296, Sep. 2000.
- [21] L. Hao and L. Xu, "Joint  $L^1$  and total variation regularization for magnetic detection electrical impedance tomography," *ACES Journal*, vol. 31, no. 6, June 2016.



**Guangdong Liu** was born in Jiangsu, China, in 1972. He received the Dr. Eng. Degree in Electromagnetic Field and Microwave Technology, from the College of Electronic Science and Engineering, Nanjing University of Posts and Telecommunications, in 2011. Currently, he is an Associate Professor of the School of Physics and Electronic Engineering, Fuyang Normal University, China. His research interests are in electromagnetic inverse scattering theory and its applications.